

# The University of Bradford Institutional Repository

<http://bradscholars.brad.ac.uk>

This work is made available online in accordance with publisher policies. Please refer to the repository record for this item and our Policy Document available from the repository home page for further information.

To see the final version of this work please visit the publisher's website. Access to the published online version may require a subscription.

**Link to publisher's version:** <http://dx.doi.org/10.1021/mp400124z>

**Citation:** Paluch KJ, Tajber L, Corrigan OI et al (2013) Impact of alternative solid state forms and specific surface area of high-dose, hydrophilic active pharmaceutical ingredients on tabletability. *Molecular Pharmaceutics*. 10(10): 3628-3639.

**Copyright statement:** This document is the Accepted Manuscript version of a Published Work that appeared in final form in *Molecular Pharmaceutics*, copyright © 2013 American Chemical Society after peer review and technical editing by the publisher. To access the final edited and published work see <http://dx.doi.org/10.1021/mp400124z>

## **Impact of alternative solid state forms and specific surface area of high-dose, hydrophilic active pharmaceutical ingredients on tabletability**

Krzysztof J. Paluch, Lidia Tajber, Owen I. Corrigan, Anne Marie Healy\*

School of Pharmacy and Pharmaceutical Sciences, Trinity College Dublin, College Green, Dublin 2, Ireland.

\* To whom correspondence should be sent. Ph.: +353 1896 1444, Fax: +353 1896 2810, e-mail: [healyam@tcd.ie](mailto:healyam@tcd.ie)

### **Abstract**

In order to investigate the effect of using different solid state forms and specific surface area ( $T_{BET}$ ) of active pharmaceutical ingredients on tabletability and dissolution performance, the mono- and dihydrated crystalline forms of chlorothiazide sodium and chlorothiazide potassium (CTZK) salts were compared to alternative anhydrous and amorphous forms, as well as to amorphous microparticles of chlorothiazide sodium and potassium which were produced by spray drying and had a large specific surface area. The tablet hardness and tensile strength, porosity and specific surface area of single-component, convex tablets prepared at different compression pressures were characterised.

Results confirmed the complexity of the compressibility mechanisms. In general it may be concluded that factors such as solid-state form (crystalline vs. amorphous), type of hydration (presence of interstitial molecules of water, dehydrates) or specific surface area of the material have a direct impact on the tabletability of the powder.

It was observed that, for powders of the same solid state form, those with a larger specific surface area compacted well, and better than powders of a lower surface area, even at relatively low compression pressures. Compacts prepared at lower compression pressures from high surface area porous microparticles presented the shortest times to dissolve, when compared with compacts made of equivalent materials, which had to be compressed at higher compression pressures in order to obtain satisfactory compacts. Therefore, NPMP materials may be considered as suitable for direct compaction and possibly for inclusion in tablet formulations as bulking agents, APIs, carriers or binders due to their good compactibility performance.

**Keywords:** solid state form, micromeritic characterisation, tabletability, dissolution

## 1. Introduction

The tabletability, defined as the capacity of powdered material to be transformed into a tablet of specified strength under the effect of compression pressure<sup>1</sup>, and the dissolution performance of an active pharmaceutical ingredient (API) in a solid dosage form may be tuned by the appropriate use of excipient materials in the formulation<sup>2</sup>. However, the possibility of using excipients such as fillers, binders, disintegrators, lubricants, solubility enhancers etc. may be limited in the case of high-dose APIs, due to the potentially large size of the final solid dosage form. In such cases the characteristics of the API have obvious importance and it is vital to assess the tabletability and dissolution performance of the API in the preformulation stage of product development.

Chlorothiazide is an example of a high dose (single oral dose: 250 mg or 500 mg), poorly water soluble API (solubility of approximately 0.2 mg/ml in water), with a very high melting point of 363 °C<sup>3</sup>. Chlorothiazide (CTZ) can form hydrophilic sodium (CTZNa) and potassium (CTZK) salts, that exist in both hydrated and anhydrous forms<sup>3,4</sup>. The amorphous form of chlorothiazide is difficult to produce, is physically unstable and prone to fast recrystallisation<sup>5,6</sup>. In contrast, sodium and potassium salts readily form amorphous forms on spray drying from solution, these forms being characterised by high-glass transition temperatures ( $T_g$ ) of 192 °C (CTZNa) and 159 °C (CTZK)<sup>7,8</sup>. In a recent study we reported on the impact of specific surface area ( $T_{BET}$ ) of nanocrystalline microparticles (NCMPs) of chlorothiazide, produced by spray drying on the tabletability performance of this poorly compactible API<sup>6</sup>. Tabletability of NCMPs was bench-marked against the reference material Di-Pac<sup>TM</sup>, as it is an excipient which is known to be a ready to-use direct compression base.

Chlorothiazide sodium and potassium salts processed by spray drying, in contrast to the parent compound, form amorphous (as opposed to crystalline) nanoparticulate microparticles (NPMPs) that are characterised by a high specific surface area (i.e. large  $T_{BET}$ ) of respectively 70 m<sup>2</sup>/g and 90 m<sup>2</sup>/g<sup>7,8</sup>.

Nanoparticulate microparticles of trehalose and raffinose were previously produced and reported by Ní Ógáin et al. (2011)<sup>9</sup>. The term NPMP refers to micron-size spheroidal particles composed of nano-sized particles, which self-assemble on spray drying.

Given that chlorothiazide salt forms can be prepared in a number of different solid states, they provide a good model for comparative tableability and dissolution studies.

Several factors that control powder compactibility have been reported to date. These factors can be organised into three main groups: particle mechanics, particle dimensions and particle adhesiveness. The most commonly reported relationships include an increase in tablet hardness with a decrease in powder particle size and greater tablet hardness as a result of greater particle shape irregularity<sup>10</sup>.

In contrast, reports on the effect on tableability of material solid state characteristics are scarce. Such solid state characteristics might include the hydration state of the material, polymorphic form or amorphousness/crystallinity. For example, a study on the influence of the crystal shape on tableability of L-lysine monohydrochloride dihydrate indicated that plate-shaped crystals formed stronger and more porous tablets in comparison to prismoidal crystals, though the effect of dehydration was not studied<sup>11</sup>. Compressed orthorhombic crystals of paracetamol, compared to the monoclinic form, exhibited greater fragmentation at low pressure, increased plastic deformation at higher pressure, and lower elastic recovery during decompression<sup>1</sup>. It was concluded, from the crystal structure, that sliding planes are present in the orthorhombic form, which could be responsible for an increase in crystal plasticity.

Maggi et al. described the tableability of  $\alpha$ -cyclodextrin ( $\alpha$ -CD) hexahydrate batches in comparison to a nonstoichiometric  $\alpha$ -CD $\cdot$ 7.57H<sub>2</sub>O form III and also partially dehydrated and amorphous forms<sup>12</sup>. Amorphous  $\alpha$ -CD samples (different batches) displayed the most suitable technological properties for use as pharmaceutical adjuvants in tableting processes, in terms of bulk and tapped density, compressibility (ability of the material to be reduced in volume as a result of applied pressure<sup>1</sup>), volume

reduction of powders, tensile strength, porosity and disintegration time of compressed tablets (produced at five different force levels, from 50 to 300 kN). A similar study by Pande and Shangraw reported a reduced compactibility (ability of the material to produce tablets of sufficient strength under the effect of densification<sup>13</sup>) performance of  $\beta$ -cyclodextrin due to dehydration<sup>13</sup>.

Trasi et al. reported that drying, and as a consequence dehydration, of glucose at high temperatures promoted the formation of amorphous regions within the particulates which were responsible for better compacting properties of processed glucose<sup>14</sup>. Sebhatu and Alderborn published a study on the relationships between the effective interparticulate contact area and the tensile strength of tablets made of amorphous (milled) and crystalline lactose of varying particle size<sup>15</sup>. Amorphous lactose produced tablets of higher tensile strength than crystalline lactose and there was a tendency for reduced particle size to increase tablet hardness. The results indicated that the differences in compactibility between amorphous and crystalline lactose are mainly the result of differences in bonding capacity, although differences in particle deformability also play a limited role.

Di Martino et al., presented a method to improve tabletability of crystalline acetazolamide by spray drying<sup>16</sup>. The study demonstrated that spray drying resulted in improved compressibility for acetazolamide, allowing for direct compression of the spray dried material, which could not be achieved with powder comprising either pure polymorph I or II. The authors attributed the improved compressibility of the spray dried material, which comprised a mixture of the two polymorphs, to greater particle rearrangement in the initial stage of compression due to its spherical habit and slightly wrinkled texture of the particle surface, favouring interparticulate bond formation.

While reports in the literature have focused on particle characteristics such as size, mechanics and adhesiveness, the impact of another physical property, namely surface area, has received less attention, with a limited number of reports investigating the impact of powder surface area on tabletability.

Westermarck et al., investigated the pore structure and  $T_{\text{BET}}$  of mannitol powder, granules and tablets and found that, the greater  $T_{\text{BET}}$ , more porous structure and the presence of a greater number of small pores resulted in increased compactibility of mannitol granules compared to mannitol powder<sup>7</sup>. Plastic deformation and fragmentation of powder and granules in compression were observed. The  $T_{\text{BET}}$  of tablets, measured by the nitrogen gas adsorption method provided a good indicator of deformation under compression. Fragmentation increased the  $T_{\text{BET}}$  of the powder, and plastic deformation decreased the  $T_{\text{BET}}$  of granules. Busignies et al. investigated changes in the  $T_{\text{BET}}$  of tablets made of microcrystalline cellulose, lactose and anhydrous calcium phosphate<sup>8</sup>. Tablets made of microcrystalline cellulose underwent plastic deformation, indicated by a reduction of  $T_{\text{BET}}$  under increased pressure. The  $T_{\text{BET}}$  of lactose tablets was found to decrease as compaction pressure was increased over 150 MPa. The  $T_{\text{BET}}$  of anhydrous calcium phosphate tablets increased regardless of the compaction pressure applied. The evolution of the  $T_{\text{BET}}$  correlated with the tensile strength of the corresponding tablets.

The present work evaluates the compactibility performance of amorphous, anhydrous nanoparticulate microparticles (NPMPs) of chlorothiazide sodium (CTZNa) and potassium (CTZK) in comparison to dihydrated CTZNa and CTZK (CTZNa DH, CTZK DH), anhydrous CTZNa and CTZK (CTZNa ANH, CTZK ANH), anhydrous amorphous spray dried microparticles (CTZNa MP, CTZK MP) and in comparison to Di-Pac™- a sugar-based direct compression excipient (Table 1). The manuscript underlines the impact of relatively high specific surface area of the previously described NPMPs<sup>7,8</sup> on tableability performance. Selected tablets are subjected to dissolution test studies in order to evaluate potential advantages of the use of NPMPs in final solid dosage forms.

## **2. Materials and methods**

### **2.1. Materials**

Materials used in experiments were chlorothiazide (CTZ) (Sigma, Ireland), sodium hydroxide (NaOH, Riedel de Haën, Germany), potassium hydroxide (KOH, Merck, Germany). Solvents and other reagents: deionised water (Purite Prestige Analyst HP, Purite Limited, UK), methanol and (Sigma, Ireland), n-propanol and ethyl acetate (Lab Scan, Ireland), butyl acetate (Merck, Germany), Hydranal-Composite and hydrochloric acid 32% (Riedel de Haën, Germany), Di-Pac™ (Domino Foods Inc., Florida, USA).

### **2.2. Methods**

#### **2.2.1. Preparation and physicochemical characterisation of different solid state forms of chlorothiazide sodium and potassium salts**

Chlorothiazide sodium (CTZNa) dihydrate and potassium (CTZK) dihydrate (DH) and anhydrous (ANH) CTZNa were prepared as previously described<sup>3,4</sup>. CTZK and CTZNa microparticles (MP) were obtained by spray drying of 2% w/v salt solution from water using the open mode configuration of the Büchi B-290 Mini Spray Dryer (Büchi, Switzerland) followed by secondary tray drying at 170 °C for 3 hours in an oven (Mettler UL 40, Germany). The same method of secondary tray drying was applied to dehydrate CTZK DH in order to obtain CTZK ANH. In order to obtain CTZK monohydrate (MH) the temperature of secondary drying was reduced to 100 °C.

Spray drying to prepare NPMP chlorothiazide sodium and potassium materials was also performed using a Büchi B-290 Mini Spray Dryer (Büchi, Switzerland). Spray dried solutions comprised a mixed solvent system of methanol and butyl acetate, as previously described<sup>7</sup>. An inert loop Büchi B-295 (for organic solvents) was used for the closed mode operation. A standard atomization nozzle with a 1.5 mm cap and 0.7 mm tip was employed for each sample. The additional, secondary drying (AD) was

performed in an incubator with forced air flow (Gallenkamp economy incubator with fan, Weiss-Gallenkamp, UK) as previously described<sup>7</sup>.

The particle size distributions of chlorothiazide sodium and potassium hydrated forms (CTZNa DH, CTZK DH and CTZK MH) and anhydrous forms (CTZNa ANH and CTZK ANH) were brought as close as possible to the size of spray dried salts using a mortar and pestle at room temperature and ambient relative humidity (RH) (35 to 40% RH), monitored using Testo<sup>TM</sup> RH and temperature data logger. The chemical purity of the produced solid-state forms was assessed using a HPLC method, as previously described<sup>8</sup>.

Materials used for tableting were comprehensively characterised as previously described<sup>7</sup>. True density ( $d_0$ ) was measured using helium (99.995% purity) with an AccuPyc 1330 Pycnometer (Micromeritics, Norcross, GA, USA) and results presented are an average of three measurements. To image particles, a Mira Variable Pressure Field Emission Scanning Electron Microscope (SEM) was used. Measurements of particle size and particle size distributions were obtained using a laser diffraction particle sizer Mastersizer 2000 (Malvern Instruments, UK). Particles were dispersed using a Scirocco dry feeder instrument with 2 bar pressure. An obscuration of 0.5-6% was obtained under a vibration feed rate of 50%; results reported are the average of three analyses. To determine the specific surface area ( $T_{BET}$ ) by the Brunauer, Emmett, Teller (BET) isotherm method, a Micromeritics Gemini VI (Micromeritics, Norcross, GA, USA) surface area analyzer was used. The amount of nitrogen adsorbed at 6 relative pressure points in the relative pressure ( $P/P_0$ ) range of 0.05 to 0.3, with an equilibration time of 10 s, was used for the BET analysis. Each average result is calculated on the basis of three measurements. Free space was determined separately for each sample using helium gas. Saturation pressure  $P_0$  was determined prior to the measurement of each sample.



### 2.2.2. Tableting and characterisation of tablets

Tablets (n=10) were compressed using an experimental, laboratory scale single punch tablet press MTCM 1 from GlobePharma (USA) supplied with an Enerpac (USA) AC RC53 piston working in the range from 0-7 GPa (max. 5 tons, 45 kN) and standard concave 10 mm diameter punch and die tooling. The die was loaded manually with a known weight (Sartorius BP121S balance) of the powder (250 mg) and compressed in the range from 21 to 278 MPa, corresponding to the range of compression force from 1 to 13 kN. The therapeutic single dose of chlorothiazide is 250 mg and may be doubled. This is one of the reasons why the weight of the tablets of chlorothiazide described in a previous study was set to the above-mentioned weight<sup>6</sup> The tablet weight was maintained at 250 mg for the current study to allow for comparisons with previously reported data on chlorothiazide tablets.

Pressure was released immediately after reaching the desired compression pressure. Tablets were pushed out of the die using the bottom punch. To lubricate the tablet press tooling, the die and upper punch were dusted, using a paint brush, with magnesium stearate.

In order to confirm that materials did not undergo solid state transformation upon compression, samples of all materials (250 mg) were subjected to compression in a Perkin Elmer hydraulic press under 10 tons load for 1 minute. The compacted discs (10 mm diameter) were subjected to PXRD analysis, then ground in an agate mortar and tested again using PXRD (data not shown).

A set of ten tablets prepared on the MTCM 1 tablet press was subjected to radial hardness testing using a Dr. Schleuniger, Pharmatron, Model 6D tablet tester. Fracture load (shear strength under compressive load) ( $P$ )<sup>19</sup> [N] was recorded for each tablet (n=10). It was monitored if the tablet capped under the applied pressure and if the breakage of the tablet occurred in a consistent manner.

The tensile strength of the materials ( $\sigma$ ) was calculated using an expanded empirical model for convex tablets<sup>19,20</sup>: equation 1.

$$\sigma_t = \frac{10P}{\pi 4r^2} \cdot 1 / \left( \frac{2.84H}{2r} - \frac{0.126H}{h} + \frac{3.15h}{2r} + 0.01 \right) \quad \text{Eqn. 1.}$$

Tablet porosity was calculated from the true density of the material ( $d_0$ ) and the density of the tablet calculated after compaction ( $d$ )<sup>12</sup>, on the basis of the measured volume.

The height (H), diameter (2r) and the band thickness (h) of the tablets were recorded (n=10) using an electronic outside micrometer IP 54 form RS (0-25 mm  $\pm$ 0.001 mm) equipped with ABS- anti crushing system. Measured geometric parameters of the tablet allowed the volume of the tablet ( $V_t$ ) to be calculated using equation 2<sup>21</sup>.

Height of the tablet (H) equals to sum of band thickness (h) and height of the tablet caps ( $h_c$ ) multiplied by 2 ( $H = h + 2h_c$ ). Therefore:  $h_c = \frac{H-h}{2}$ . Volume of the caps forming tablet equals to:  $V_c = \frac{\pi}{3}(3r^2 + h_c^2)h_c$ . Volume of the cylinder forming tablet equals to:  $V_{cyl} = \pi r^2 h$ . Therefore,  $V_t$  equals to:

$$V_t = \frac{\pi}{3}(3r^2 + h_c^2)h_c + \pi r^2 h \quad \text{Eqn.2.}$$

Materials used for tableting are listed in Table 1.

Table 1. Description of materials used for tableting studies.

Abbreviation	Description of system
<b>CTZNa DH</b>	Crystalline chlorothiazide sodium dihydrate
<b>CTZNa ANH</b>	Anhydrous chlorothiazide sodium
<b>CTZNa MP</b>	Spray dried nonporous microparticles of amorphous, anhydrous chlorothiazide sodium
<b>CTZNa NPMP</b>	Spray dried nanoparticulate microparticles of amorphous, anhydrous chlorothiazide sodium
<b>CTZK DH</b>	Crystalline chlorothiazide potassium dihydrate
<b>CTZK MH</b>	Particles of crystalline chlorothiazide potassium monohydrate
<b>CTZK ANH</b>	Particles of amorphous chlorothiazide potassium
<b>CTZK MP</b>	Spray dried nonporous microparticles of amorphous, anhydrous chlorothiazide potassium
<b>CTZK NPMP</b>	Spray dried nanoparticulate microparticles of amorphous, anhydrous chlorothiazide potassium

<b>Di-Pac™</b>	Direct compacting and tableting sugar: 96.5±1.5% sucrose, 3.0±0.75% maltodextrin
----------------	--

### 2.2.3. Dissolution studies

Dissolution studies were performed with a type 2 dissolution test apparatus (VanKel VK7000 dissolution test station equipped with a VK650 heater/circulator)<sup>19</sup>. The rotation speed of the paddle was set to 50 rpm. 900 ml of degassed phosphate buffer pH 6.8<sup>19</sup> was used as the dissolution medium, equilibrated at 37 °C. The dissolution medium was constantly circulated using an LSMatec peristaltic pump fitted with a 10 µm cannula filter (HMWPE, Porex Technologies, Germany) through a 2 mm flow-through UV cuvette placed in a Cecil CE2020 UV-spectrophotometer set to measure absorbance at  $\lambda=265$  nm. The rate of medium circulation was set to 25 ml/min. Presented results are an average of at least three measurements.

### 2.2.4. Statistical analysis of data

Statistical analysis was carried out using Minitab (State College, PA, USA) software. A t-test at a significance level of 0.05 was applied, with a p value of less than 0.05 indicating that the observed differences between the means were statistically significant.

## 3. Results and Discussion

### 3.1. Physicochemical characterisation of powders subjected to compaction

The crystal structures of the chlorothiazide sodium dihydrate (CTZNa DH) and its alternative anhydrous (CTZNa ANH) form were previously described<sup>1</sup>. The true density and specific surface area,

determined by BET analysis ( $T_{\text{BET}}$ ), of all materials are listed in Table 2, while the particle size distributions of all materials subjected to tableting are shown in Table 3. HPLC indicated that there was no chemical degradation in any of the solid state forms produced by the methods described in section 2.2.1. As described previously, amorphous materials of chlorothiazide sodium and chlorothiazide potassium were physically and chemically stable under long term stability study storage conditions (RH  $\approx$ 0%, 25 °C) for over six months<sup>8</sup>. After compaction in the IR press (as described in section 2.2.2.), none of the tested materials showed a change in surface or bulk solid state characteristics in comparison to the starting powders.

Table 2. Micromeritic properties of powders which were subjected to compaction (true density ( $d_0$ ), specific surface area by BET ( $T_{\text{BET}}$ ), and specific surface area calculated from laser diffraction particle size analysis data ( $T_{\text{LD}}$ ) based on surface weighted mean ( $d[3,2]$ ). Abbreviations as per Table 1.

<b>Material</b>	<b>True density <math>d_0</math> [g/cm<sup>3</sup>]</b>	<b><math>T_{\text{BET}}</math> [m<sup>2</sup>/g]</b>	<b><math>T_{\text{LD}}</math> [m<sup>2</sup>/g]</b>
<b>CTZNa DH</b>	1.728 $\pm$ 0.004	2.73 $\pm$ 0.01	1.41 $\pm$ 0.02
<b>CTZNa ANH</b>	1.883 $\pm$ 0.001	3.07 $\pm$ 0.01	1.04 $\pm$ 0.03
<b>CTZNa MP</b>	1.837 $\pm$ 0.015	1.32 $\pm$ 0.04 <sup>(a)</sup>	1.82 $\pm$ 0.01
<b>CTZNa NPMP</b>	1.856 $\pm$ 0.001	72.32 $\pm$ 0.71 <sup>(a)</sup>	1.81 $\pm$ 0.02
<b>CTZK DH</b>	1.887 $\pm$ 0.003	0.62 $\pm$ 0.03	0.72 $\pm$ 0.04
<b>CTZK MH</b>	1.859 $\pm$ 0.001	1.74 $\pm$ 0.03	0.83 $\pm$ 0.03
<b>CTZK ANH</b>	1.881 $\pm$ 0.003	1.30 $\pm$ 0.02	0.94 $\pm$ 0.01
<b>CTZK MP</b>	1.872 $\pm$ 0.003	1.33 $\pm$ 0.01 <sup>(a)</sup>	1.61 $\pm$ 0.02
<b>CTZK NPMP</b>	1.863 $\pm$ 0.012	90.20 $\pm$ 0.91 <sup>(a)</sup>	1.71 $\pm$ 0.02
<b>Di-Pac<sup>TM</sup></b>	1.554 $\pm$ 0.001	0.21 $\pm$ 0.04 <sup>(b)</sup>	0.11 $\pm$ 0.01

a) and b) - results consistent with values previously reported<sup>6,7</sup>.

Table 3. Particle size distribution parameters of tested powders: 10<sup>th</sup> percentile particle size (d(10)),

median particle size (d(50)), 90<sup>th</sup> percentile particle size (d(90)) and Span:  $Span = \frac{d(90) - d(10)}{d(50)}$ .

Sample	d(10)	d(50)	d(90)	Span	Particle size distribution
CTZNa DH	0.92±0.02	5.44±0.13	53.11±0.10	9.64±0.21	Trimodal
CTZNa ANH	1.31±0.12	6.22±0.32	49.40±0.24	7.70±0.34	Trimodal
CTZNa MP	1.43±0.21	2.61±0.11 <sup>(a)</sup>	7.24±0.13	1.80±0.10 <sup>(a)</sup>	Monomodal
CTZNa NPMP	1.11±0.10	2.93±0.02 <sup>(a)</sup>	6.8±0.22	1.91±0.14 <sup>(a)</sup>	Monomodal
CTZK DH	1.30±0.11	8.73±0.14	58.42±0.22	6.61±0.22	Trimodal
CTZK MH	1.30±0.23	5.24±0.22	16.82±0.14	3.02±0.12	Bimodal
CTZK ANH	1.72±0.14	9.70±0.21	113.41±0.32	11.63±0.31	Bimodal
CTZK MP	1.23±0.12	3.11±0.13 <sup>(a)</sup>	6.64±0.21	1.82±0.23 <sup>(a)</sup>	Monomodal
CTZK NPMP	1.03±0.02	3.12±0.13 <sup>(a)</sup>	6.84±0.01	1.91±0.13 <sup>(a)</sup>	Monomodal
Di-Pac™	27.31±0.31	178.44±0.63 <sup>(b)</sup>	398.51±1.22	2.11±0.10	Monomodal

a) and b) - results consistent with values previously reported<sup>6,7</sup>.

CTZNa DH had a true density ( $d_v$ ) of 1.728±0.004 g/cm<sup>3</sup> compared to a theoretical density, calculated based on the single crystal X-ray diffraction data, of 1.836 g/cm<sup>3</sup>. Surface area by BET analysis ( $T_{BET}$ ) of CTZNa DH was measured to be 2.73±0.01 m<sup>2</sup>/g. In comparison to CTZNa DH, CTZNa ANH which was size reduced with a mortar and pestle had a higher  $d_v$  of 1.883±0.001 g/cm<sup>3</sup>, which may be attributed to rearrangement of the crystal lattice due to dehydration. The  $T_{BET}$  of this CTZNa ANH sample was 3.07±0.01 m<sup>2</sup>/g.

Properties of spray dried systems of CTZNa which were amorphous, anhydrous and consisting of nonporous microparticles (CTZNa MP) and CTZNa systems which were amorphous, anhydrous and consisting of nanoparticulate microparticles (CTZNa NPMP) were previously described<sup>8</sup>. Both spray dried materials, CTZNa MP and CTZNa NPMP, were anhydrous and presented values of true density close to that of CTZNa ANH, i.e. 1.837±0.015 g/cm<sup>3</sup> and 1.856±0.001 g/cm<sup>3</sup>, respectively, for CTZNa

MPs and CTZNa NPMP. As both materials after spray drying were fully PXRD amorphous<sup>7,8</sup>, a slight decrease in the true density values in comparison to CTZNa ANH was not surprising, since amorphisation results in a decrease in true density in comparison to the crystalline material<sup>2</sup>. Particle size analysis by laser diffraction determined a monomodal particle size distribution with a median particle size of  $2.6\pm0.1\ \mu\text{m}$  and  $2.9\pm0.0\ \mu\text{m}$  for MPs and NPMPs, respectively. The  $T_{\text{BET}}$  of NPMPs confirmed an increase in surface area of the material in comparison to CTZNa MPs, as was expected due to the porosity of the spray dried NPMP particles which was observed on SEM (Fig. 1a);  $T_{\text{BET}}$  for the NPMP system was  $72.32\pm0.71\ \text{m}^2/\text{g}$ , in contrast to a  $T_{\text{BET}}$  of  $1.32\pm0.04\ \text{m}^2/\text{g}$  for the smooth spheroidal particles of CTZNa MPs<sup>7</sup>.

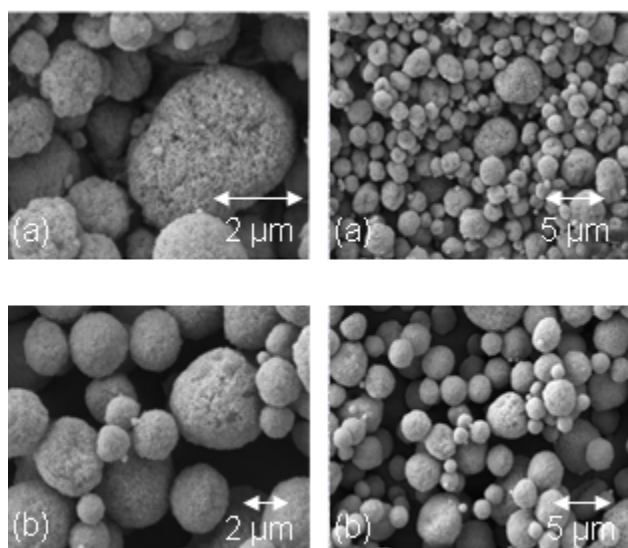


Fig. 1. SEM images of NPMP a) CTZNa<sup>3</sup>, b) CTZK<sup>3</sup>.

The crystal structure of chlorothiazide potassium dihydrate (CTZK DH) and alternative solid state forms of the potassium salt, i.e. the monohydrate (CTZK MH) and the anhydrous form were previously described<sup>4</sup>. The true density of CTZK DH material was  $1.887\pm0.003\ \text{g}/\text{cm}^3$ , which is close to the theoretical value calculated based on the single crystal X-ray diffraction data of  $1.867\ \text{g}/\text{cm}^3$ . The

$T_{\text{BET}}$  of CTZK DH was  $0.62 \pm 0.03 \text{ m}^2/\text{g}$ , while that of CTZK MH was measured to be  $1.74 \pm 0.03 \text{ m}^2/\text{g}$ . The difference in surface area between the two hydrated states may be attributed to irregularities of morphology and empty voids formed due to the loss of crystal water. The anhydrous material, CTZK ANH, had a  $d_0$  of  $1.881 \pm 0.003 \text{ g}/\text{cm}^3$ , a median particle size,  $d(50)$ , of  $9.7 \pm 0.2 \text{ }\mu\text{m}$  and a  $T_{\text{BET}}$  of  $1.30 \pm 0.02 \text{ m}^2/\text{g}$ . The  $T_{\text{BET}}$  of CTZK MP, which comprised spheroidal microparticles with slightly crumpled surfaces<sup>7</sup>, was  $1.33 \pm 0.01 \text{ m}^2/\text{g}$  and was  $\sim 70$ -times lower than that of the CTZK NPMP material ( $90.20 \pm 0.91 \text{ m}^2/\text{g}$ , Fig. 1b).

Di-Pac<sup>TM</sup> was selected as a comparator material in this study as it is a crystalline filler/binder used as a direct compression base<sup>6</sup>. Di-Pac<sup>TM</sup> had the lowest measured  $T_{\text{BET}}$  of the materials measured at  $0.21 \pm 0.04 \text{ m}^2/\text{g}$ .

In this work we sought to minimise the differences in particle size (reflected in the  $d(10)$  and  $d(50)$  values) among powders subjected to tabletability studies, such that the impact of solid state and morphological changes, as opposed to particle size could be evaluated. Particle size distribution was reported to have a limited impact on tensile strength of tablets made of sodium chloride and sucrose, where wide, narrow and bimodal particle distributions of particles with median particle size of about  $400 \text{ }\mu\text{m}$  were investigated<sup>23</sup>. The particles of CTZ salts did not vary considerably in  $d(10)$  size values, ranging from  $0.9$  to  $1.7 \text{ }\mu\text{m}$  in comparison to  $27 \text{ }\mu\text{m}$  for Di-Pac<sup>TM</sup> (Table 3). The range of  $d(50)$  was also narrow, from  $2.6$  to  $9.7 \text{ }\mu\text{m}$  versus  $178 \text{ }\mu\text{m}$  for Di-Pac<sup>TM</sup>.

## **3.2. Assessment of tabletability performance**

### **3.2.1. Tablet hardness (P) and tensile strength ( $\sigma$ )**

If the powder bed forming the tablet has good compactibility performance, it is expected that the desired hardness (P) of the tablet (here referred to as force to tensile failure<sup>19</sup>) will be reached using

relatively low compression pressure. Furthermore, the hardness of the tablet will not vary significantly under fluctuations of the preset compression pressure during processing, and the change of the tablet hardness will be responsive to the change of compression pressure. In contrast to the tablet hardness (P), which is directly related to tablet shape and size, the tensile strength ( $\sigma$ ) may be compared for different tablet sizes and shapes<sup>19,20</sup>.

As an example of compactibility performance of a pure pharmaceutical excipient designed for direct compression, Di-Pac™ formed tablets at a compression pressure as low as 64 MPa, which had a hardness of 23.7 N. The hardness increased linearly with compression pressure at a rate of 1.12 N per 1 MPa<sup>6</sup>.

Of the CTZNa systems studied, the material with the best compactibility performance in terms of tensile strength versus compression pressure was CTZNa NPMP (Fig. 2a).



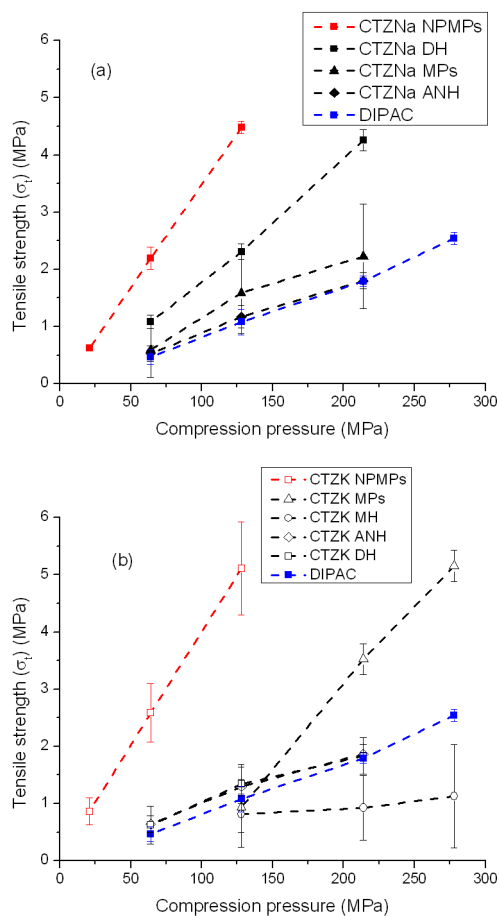


Fig. 2. a) Tensile strength ( $\sigma_t$ ) in relation to compression pressure for: CTZNa DH, CTZNa ANH, CTZNa MPs, CTZNa NPMP and Di-Pac™ and b) for CTZK DH, MH and ANH, CTZK MP and CTZK NPMP. Error bars express standard deviation (SD) for comparison purposes.

The corresponding profile of change of compression pressure versus tensile failure for this system is presented in the supporting information file (Fig. SI.1a). At a compression pressure of 21 MPa CTZNa NPMPs formed tablets with a  $\sigma_t$  of 0.62 MPa. For every unit increase of compression pressure, the  $\sigma_t$  value of the CTZNa NPMP material increased by  $36 \times 10^{-3}$  MPa, which was the greatest dependence of

$\sigma_t$  on compression pressure for all CTZNa materials tested; this was compared to an increase in the  $\sigma_t$  value of  $9.5 \times 10^{-3}$  MPa for every unit increase in compression pressure for Di-Pac™. Other CTZNa materials did not undergo compaction at a compression pressure of 21 MPa. Attempts to compress these materials (other than NPMPs) under compression pressures lower than 21 MPa resulted in tablets falling apart upon ejection from the die. The  $\sigma_t$  at a compression pressure of 64 MPa for CTZNa DH was 1.08 MPa and was significantly ( $p < 0.05$ ) higher than the equivalent values recorded for Di-Pac™ (0.47 MPa), CTZNa ANH (0.53 MPa) and CTZNa MPs (0.59 MPa). The  $\sigma_t$  versus compression pressure profiles for CTZNa tablets are similar to those of P versus compression pressure (Fig. SI.1a). The supporting information file Table SI.1 contains a compilation of all parameters of the tablets discussed below in relation to the compression pressure applied.

As was previously observed for CTZ, spray drying from mixed solvent systems resulted in powders (i.e. NPMPs) with improved compactibility compared to micronised materials<sup>6</sup>. The fact that CTZNa DH showed a better compactibility performance than CTZNa ANH or CTZNa MPs may be ascribed to the presence of water molecules in the crystal lattice of CTZNa DH. A similar phenomenon was noted by Sun and Grant who investigated the impact of compaction pressure on the tensile strength of tablets of anhydrous and monohydrated p-hydroxybenzoic acid, and reported that water of crystallisation improves tableting properties of p-hydroxybenzoic acid<sup>24</sup>. Pande and Shangraw also reported a reduced compactibility performance of dehydrated  $\beta$ -cyclodextrin in comparison to the hydrated material<sup>13</sup>. In the current work, it was observed that, on average, the tensile strength of tablets made of CTZNa DH was greater than the tensile strength of tablets made of CTZNa ANH for tablets compressed at the same pressure.

It is hypothesised here that the water molecules contained in the crystal lattice cause the particles of CTZNa DH powder to stick together upon the application of compression pressure, thus

producing tablets with a greater  $\sigma_i$  in comparison to those made of the dehydrated material (CTZNa ANH) in which only plastic deformation, crushing, interlocking or thermal fusion of molecules can occur. Based on the results of crystallographic studies and the fact that the PXRD pattern of compressed CTZNa DH did not change in comparison to the starting material, it was surmised that it was not the coordinated molecules of water, but the interstitial water that may be responsible for the better compactibility of CTZNa DH compared to the anhydrous form. This is supported by extensive studies involving dynamic vapour sorption of water and the impact of absorbed water on the PXRD pattern of CTZNa DH, as previously described<sup>1</sup>.

CTZNa ANH and CTZNa MPs tablets had lower  $\sigma_i$  at respective compression pressures than tablets of CTZNa DH (Fig. 2a). It should be noted that the anhydrous and amorphous CTZNa system (CTZNa MP) prepared by spray drying compacted better than CTZNa ANH (i.e. the equivalent crystalline material). At a compression pressure of 128 MPa, tablets formed from CTZNa MPs had a tensile strength of 1.59 MPa, while the tablets made of CTZNa ANH material had a  $\sigma_i$  of only 1.17 MPa. This improvement may be attributed to the change of the solid state form, since the MPs produced by spray drying were amorphous, but CTZNa ANH still contained a residual crystalline phase. This indicates that the presence of an amorphous phase may have more importance in terms of influencing tabletability performance over the small differences in  $T_{BET}$  between tested materials.

Analysis of the profiles of  $\sigma_i$  versus compression pressure for CTZK materials (Fig. 2b) allowed similar conclusions to be drawn to those made for the equivalent CTZNa systems with respect to tabletability; the best compactibility performance being demonstrated for the spray dried materials, CTZK NPMP and CTZK MP. The profiles of  $\sigma_i$  versus compression pressure for the CTZK systems were similar to those showing relationships between  $P$  and compression pressure which are presented in Fig. SI.1b (in the supplementary file). Tablets made of CTZK NPMP at 21 MPa compression

pressure had a slightly higher  $\sigma_c$  (0.86 MPa) than the equivalent CTZNa system (0.62 MPa). The  $\sigma_c$  increased to 2.58 MPa and 5.11 MPa, respectively, at 64 MPa and 128 MPa compression pressures for CTZK NPMP.

Tablets made of CTZK MPs showed a similar change in  $\sigma_c$  with increasing compression pressure as the CTZK NPMP system, with  $\sigma_c$  increasing by  $28.3 \times 10^{-3}$  MPa and  $39.6 \times 10^{-3}$  MPa for every MPa increase in compression pressure, for the MP and NPMP system, respectively. The lowest change in  $\sigma_c$  with increasing compression pressure was found for tablets made of CTZK MH, with  $\sigma_c$  changing by  $2.10 \times 10^{-3}$  for every MPa increase in compression pressure. The tensile strength of this batch of tablets was in the range from 0.81 MPa to 1.13 MPa at compression pressures between 128 MPa and 278 MPa. Amorphous CTZK MPs had better tableability than CTZK DH, CTZK MH and CTZK ANH. Over a compression pressure range of 64-128 MPa, the change of  $\sigma_c$  for CTZNa MPs was smaller (from 0.59 to only 1.59 MPa) than for CTZK MPs (0.93 to 3.52 MPa). The change in the  $\sigma_c$  for CTZNa MPs was lower than for amorphous lactose<sup>35</sup>, while the values for CTZK MPs were in a comparable range. This may be attributed to the lower Tg of CTZK (~159 °C) compared to CTZNa (~192 °C)<sup>7</sup>. It may be hypothesised that at high pressures, under mechanical and thermal stress which occur upon compaction, in the small areas of contact points between amorphous particles, lower Tg materials will be more prone to fusion, resulting in better compactibility. Amorphous lactose has a relatively low Tg (~ 105 °C)<sup>35</sup>. Drying, and as a consequence dehydration, of glucose at high temperatures was reported to promote the formation of amorphous phases which were responsible for better compacting properties of processed glucose<sup>34</sup>. These conditions are similar to the conditions of production of amorphous and anhydrous CTZK MPs and CTZK ANH, where the temperature of final drying was higher (170 °C) than the Tg of CTZK (159 °C)<sup>7</sup> which could result in a partial amorphisation of CTZK ANH.

No increase in the  $\sigma_c$  of compacts made of CTZK DH in comparison to those made of the anhydrous CTZK ANH form was seen. This may be a result of the presence of an amorphous content in CTZK ANH or it may be due to the lack of interstitial molecules of water in the crystal structure of CTZK DH<sup>4</sup>. The presence of interstitial water was related to a high tensile strength in the case of CTZNa DH tablets.

The lowest change of  $\sigma_c$  in relation to compression pressure applied was observed for CTZK MH tablets and this may be related to two aspects. Firstly, it is unlikely that the water molecules in CTZK MH are placed interstitially<sup>4</sup>. The other factor is related to the reduced possibility of amorphisation of CTZK MH in comparison to anhydrous CTZK ANH form, as the drying temperature of CTZK DH resulting in the CTZK MH form is approximately 80 °C below the T<sub>g</sub> of the amorphous form of CTZK.

### **3.2.2 Tablet porosity ( $\epsilon_v$ ) and surface area (T<sub>BET</sub>)**

The porosity of the tablet ( $\epsilon_v$ ) is a relative measure of empty spaces in the volume of the tablet in relation to the true density ( $d_v$ ) of the compressed material. The density of a completely compressed tablet with 0%  $\epsilon_v$  will be equal to the  $d_v$  of the powder that forms the tablet. Porosity is one of the measures of compressibility performance of the material under applied compression pressure<sup>4</sup>.

The calculated  $\epsilon_v$  of the CTZNa NPMP tablets at a compression pressure of 21 MPa was 64.51% (Fig. 3a); under a compression pressure of 64 MPa this decreased to 46.67% and reached 31.97% at 128 MPa.

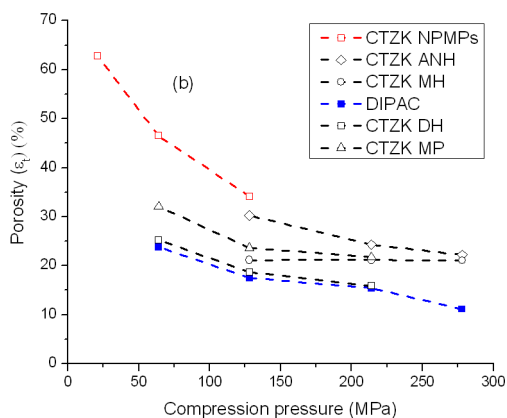
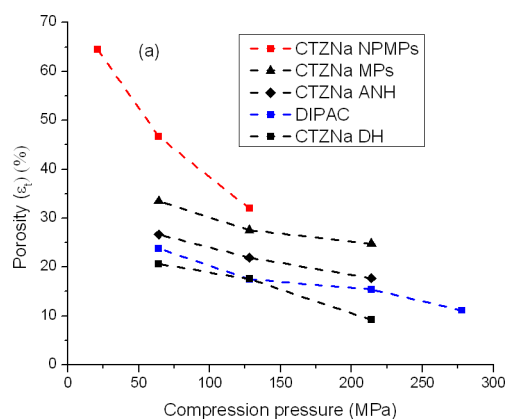


Fig. 3. a) Porosity of the tablet ( $\epsilon_t$ ) in relation to compression pressure for: CTZNa DH, ANH, CTZNa MP, CTZNA NPMP and Di-Pac™, b) CTZK DH, MH and ANH, CTZK MP, CTZK NPMP compared to Di-Pac™.

Over the range of compression pressures analysed, the  $\epsilon_t$  of the NPMP tablets reduced by about 32.54% gaining 3.86 MPa in the tablet  $\sigma_t$ . The tablets made of nonporous materials tested over a range of compression pressure from 64 MPa to 214 MPa did not present such large variations in tablet porosity. Among the nonporous systems, the largest  $\epsilon_t$ , of 33.5% at 64 MPa, was recorded for CTZNa MP tablets. CTZNa ANH and CTZNa DH tablets made at 64 MPa compression pressure had  $\epsilon_t$  of 26.67% and 20.63%, respectively. CTZNa DH, CTZNa ANH and CTZNa MP materials had similar

responsiveness in terms of change in  $\epsilon$  with increasing compression pressure, but the dihydrated material presented a much better performance in terms of the increase of tensile strength, which was similar to the NPMP system.

The largest change of  $\epsilon$  versus increasing compression pressure was recorded for the CTZK NPMP tablets (Fig. 3b). The change of  $\epsilon$  was very similar to that of the equivalent CTZNa NPMP compacts. The CTZK NPMP tablets compressed at 21 MPa compression pressure had a  $\epsilon$  of 62.79%. After the compression of the powder at 128 MPa the  $\epsilon$  was reduced to 34.17%. In the tested range of compression pressures from 21 up to 128 MPa CTZK NPMP tablets lost 28.62% of  $\epsilon$ , while the  $\sigma$  increased by 4.25 MPa. When analysing tablets of other CTZK materials, at 128 MPa compression pressure, the largest  $\epsilon$  of 32.07%, was recorded for the nonporous spray dried material (CTZK MPs). The  $\epsilon$  of tablets made of CTZK ANH, CTZK MH and CTZK DH decreased with an increased degree of material hydration and was 24.31%, 21.13% and 18.71%, respectively. The same order was maintained at 214 MPa compression pressure. A reduction of  $\epsilon$ , by only 0.07%, over the tested range of compression pressures from 128 to 278 MPa was recorded for CTZK MH material. This change in  $\epsilon$  corresponded to a very small, but a statistically significant ( $p < 0.05$ ) change of tablet  $\sigma$ , of 0.32 MPa, indicating that this material presented the worst compactibility, regarding reduction of  $\epsilon$  and increase of  $\sigma$  with the change of compression pressure, of all the powders tested.

In comparison, over the range from 64 to 214 MPa compression pressure, the tablet porosity of Di-Pac™ (Fig. 3a) decreased by about 8.38%, while the tablet tensile strength increased by about 1.33 MPa. Compilation of the obtained results of  $\epsilon$  and corresponding  $\sigma$  (Fig. 4) confirms the superior compactibility properties of anhydrous and amorphous CTZNa and CTZK NPMP systems compared to other materials examined.

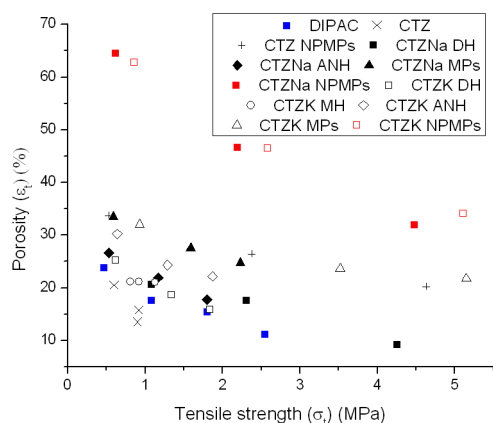


Fig. 4. Porosity of the tablet in relation to tensile strength, for all tablets produced<sup>4</sup>.

At each data point corresponding to a particular compression pressure, NPMP systems presented greater  $\sigma_t$  and  $\epsilon$ , when compared to the rest of the systems tested. Porosities of CTZK NPMP and CTZNa NPMP tablets (at a given compression pressure) are very similar; however CTZK NPMP tablets tend to have slightly higher  $\sigma_t$  values.

The  $\epsilon$  of NPMP tablets was seen to be reduced with increasing compression pressure and at 128 MPa was close to values of  $\epsilon$ , for tablets made of non-porous materials, at about ~30%. The porosity of tablets may not reflect changes in the  $T_{BET}$  of compressed materials. In order to evaluate changes of  $T_{BET}$  of the compressed materials, tablets were subjected to BET analysis. It was hypothesised that this analysis would help to elucidate particular compaction mechanisms in the production of NPMP tablets. The mechanisms expected to enlarge  $T_{BET}$  of the material are crushing and plastic deformation. The one mechanism, which will result in a reduction in  $T_{BET}$  is fusion of particles into larger agglomerates. Interlocking of particles or elastic deformation under compression are considered as compaction mechanisms which do not have an impact on the  $T_{BET}$  of the tablets<sup>7</sup>. Under increasing compression pressure the bed of powder placed in the die between the upper and lower punches starts to compact



firstly by migration of powder and interlocking<sup>7</sup>. Secondly, elastic deformation can occur with increasing compression pressure; this elastic deformation may transfer into a permanent change of particle shape, i.e. plastic deformation. A further increase of compression load may result in particle cracking and crushing, together with the same processes as those occurring at lower loads. Finally, under high compression pressure, smaller particles can merge (fuse) together into larger particles.

The analysis of the  $T_{\text{BET}}$  values of CTZNa ANH at the first compression pressure point revealed fusion of the material, as the  $T_{\text{BET}}$  decreased from 3.07 m<sup>2</sup>/g (loose powder) to 2.61 m<sup>2</sup>/g (tablet compressed at 64 MPa compression pressure) (Fig. 5).

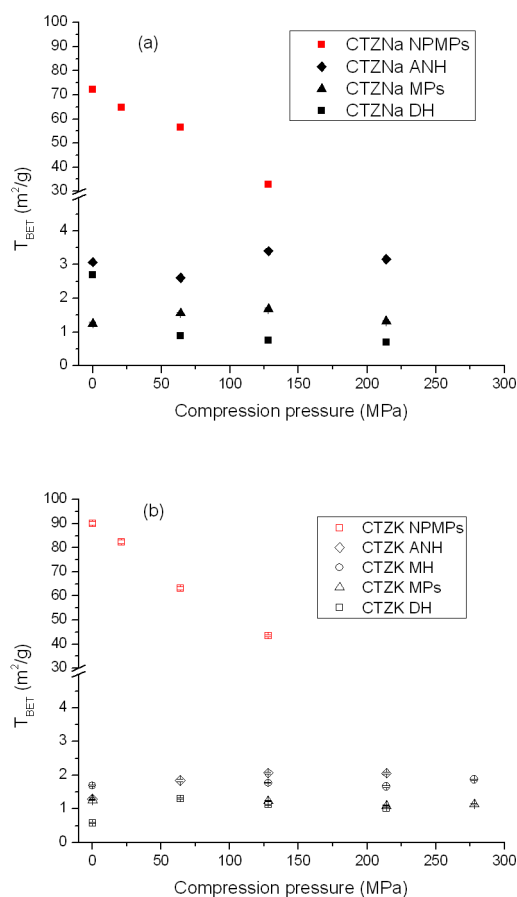


Fig. 5. Specific surface area of the tablet ( $T_{\text{BET}}$ ) in relation to compression pressure for: a) CTZNa DH, CTZNa ANH, CTZNa MP and CTZNa NPMP, b) CTZK DH, MH and ANH MP, CTZK MP and CTZK NPMP.

This behaviour upon compression may be ascribed to the layered (foliated) structure of CTZNa ANH particles, seen on SEM pictures (Fig. 6c), similar to slate rock. Foliation of particles of the CTZNa DH form was not observed (Fig. 6a).

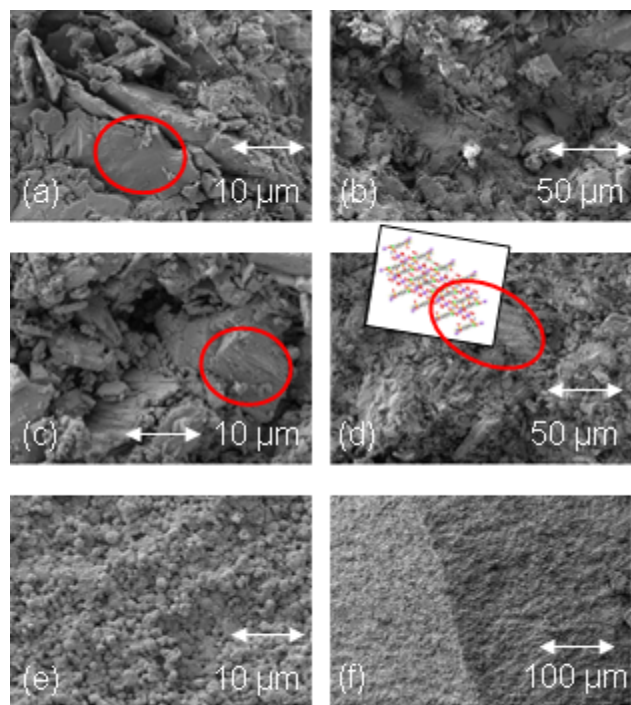


Fig. 6. SEM images of: a) morphology of CTZNa DH, b) cross section of the tablet made of CTZNa DH compressed at 128 MPa, c) morphology of CTZNa ANH, d) cross section of the tablet made of CTZNa ANH compressed at 128 MPa with an insert depicting the crystal lattice packing of CTZNa DH, e) and f) cross section of the tablet made of CTZNa NPMP compressed at 128 MPa. Red circles indicate occurrence of foliation in CTZNa ANH possibly related to evaporation of water from CTZNa DH crystal structure (in inset).

Foliation may be ascribed to evaporation of water molecules layered along the *a* axis in the crystal structure of CTZNa DH<sup>1</sup>. The reduction of  $T_{\text{BET}}$  at the initial compression pressure of 64 MPa may be

assigned to compression of the crystal lattice of CTZNa ANH. At a compression pressure of 128 MPa  $T_{\text{BET}}$  increased in comparison to that of the loose powder, to 3.4 m<sup>2</sup>/g, indicating the possibility of cracking (Fig. 6b) of particles, and then slightly dropped to 3.16 m<sup>2</sup>/g at a compression pressure of 214 MPa, where particles may have started to fuse.

In contrast to CTZNa ANH, CTZNa DH showed a constant drop of  $T_{\text{BET}}$  from the value presented for the loose powder (2.69 m<sup>2</sup>/g) to 0.89 m<sup>2</sup>/g at the compression pressure of 64 MPa and to 0.7 m<sup>2</sup>/g at the compression pressure of 278 MPa. This indicated that particles of this system fused together very easily even at low compression pressure, possibly due to the release of molecules of interstitial crystal water, as discussed above. The change in the  $T_{\text{BET}}$  values of tablets made of CTZNa MPs was similar to that recorded previously for CTZ NPMP, where firstly particles started to crack and break, increasing  $T_{\text{BET}}$  slightly, a plateau was reached between 64 and 128 MPa and then the  $T_{\text{BET}}$  dropped at 214 MPa compression pressure suggesting fusion of particles<sup>6</sup>.  $T_{\text{BET}}$  reduction under increasing compression pressure recorded for the CTZNa NPMP indicated that particles of this system compacted predominantly due to the fusion of particles, regardless of the compaction pressure.

In the compression pressure range of 21 MPa to 128 MPa, the reduction in  $T_{\text{BET}}$  versus compression pressure for the CTZK NPMP tablets was approximately linear and similar in behaviour to the CTZNa NPMPs. The change in  $T_{\text{BET}}$  for CTZK MH and CTZK MPs tablets on rising compression pressure was very low, indicating that these systems were compacted predominantly due to elastic deformation and interlocking. CTZK ANH material behaved similarly to Di-Pac<sup>TM</sup>, but differently to the equivalent CTZNa ANH system. CTZK ANH did not present a  $T_{\text{BET}}$  drop at the initial compression pressure, which may be ascribed to the different crystal structure of the hydrate, where, in contrast to CTZNa, chlorine atoms of CTZ are involved in direct coordination bonds with the potassium cation, as was presented previously<sup>3</sup>, which may prevent foliation, as described for CTZNa ANH.

Comparisons of the  $T_{\text{BET}}$  values with porosity data (Fig. 7 a) of the tablets for all systems tested indicated that the CTZK and CTZNa NPMP materials formed highly-porous tablets with large  $T_{\text{BET}}$ . The high porosity could be visualised by SEM (Fig. 6f).

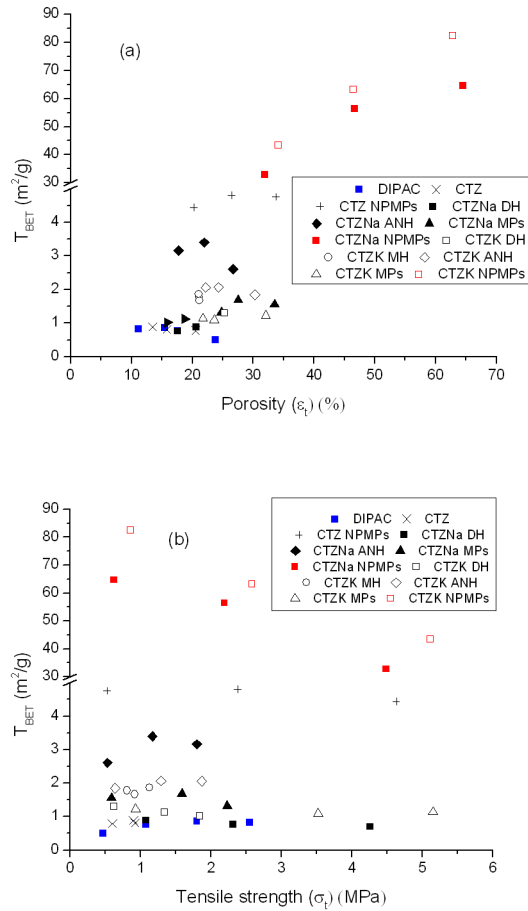


Fig. 7. Specific surface area of the tablet ( $T_{\text{BET}}$ ) versus: a) tablet porosity ( $\epsilon_t$ ) and versus: b) tablet tensile strength ( $\sigma_t$ ).

NPMP tablets, despite undergoing compression and reaching porosities comparable to those determined for tablets made of non-NPMP materials, still preserved relatively high  $T_{\text{BET}}$ . Furthermore, the NPMP tablets had the greatest mechanical strengths, as seen from the  $T_{\text{BET}}$  versus  $\sigma_t$  plots (Fig. 7b). The  $\sigma_t$  of NPMP tablets was comparable or higher than the  $\sigma_t$  of tablets made from conventionally produced materials at similar  $T_{\text{BET}}$  values.

Overall, tablets made of NPMPs were characterised by the best compactibility. These tablets presented the highest  $\sigma_c$  at low compression pressure compared to other tablets. The highest  $\sigma_c$  corresponded with the highest  $\epsilon_c$  and the highest  $T_{BET}$  of the material in the tablet form after compression. In the study of Sebhatu and Alderborn on relationships between the effective interparticulate contact area and the  $\sigma_c$  of tablets made of amorphous and crystalline lactose, the  $\epsilon_c$  made of the amorphous material was similar to that made of crystalline lactose and was  $\sim 30\%$  at a compression pressure of 75 MPa and decreased to  $\sim 20\%$  at 125 MPa ( $0.2\%/MPa$ )<sup>13</sup>. For the amorphous systems the decrease in  $\epsilon_c$  corresponded with an increase in the  $\sigma_c$  from 0.5 MPa to approximately 3 MPa, while the  $\sigma_c$  of tablets made of crystalline lactose increased only in a range from 0.2 to nearly 1 MPa. In comparison, the  $\epsilon_c$  of the CTZNa and CTZK NPMP materials varied in this compression pressure range from  $\sim 47\%$  to  $\sim 32\%$ . These higher values of  $\epsilon_c$  in comparison to the reported lactose tablets corresponded to a greater change and range of  $\sigma_c$  from 2.2 MPa to as high as 5.1 MPa.

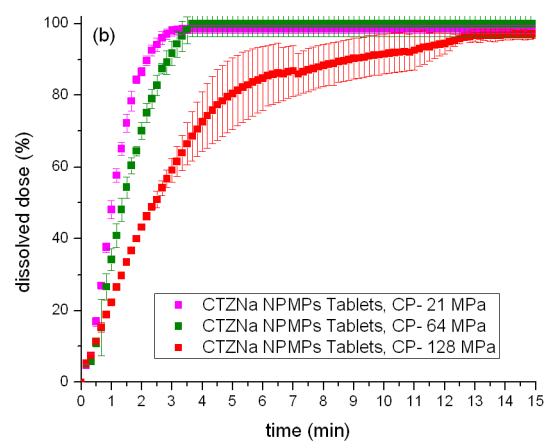
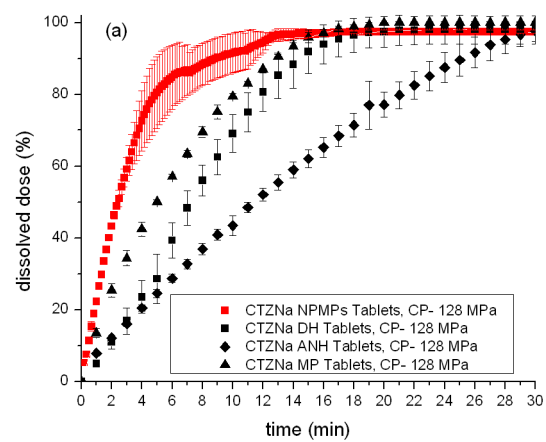
In the study of Westermarck et al. the pore structure and  $T_{BET}$  of tablets made of mannitol powder and processed granulate were compared<sup>15</sup>. The  $\epsilon_c$  of mannitol powder tablets decreased from 21% to 14% over a compression pressure range from 72 up to 196 MPa. The decrease of  $\epsilon_c$  corresponded to an increase in  $T_{BET}$  of the tablet from 0.58 to 0.61 m<sup>2</sup>/g in comparison to the initial  $T_{BET}$  of the powder of 0.34 m<sup>2</sup>/g. The reported increase of  $T_{BET}$  for mannitol tablets was similar to that observed for CTZK ANH tablets, ascribed to the mechanism of brittle fracture of particles with rising compression pressure. The reduction of  $\epsilon_c$  (26%-17%) for tablets made of mannitol granulate, in contrast to tablets made of the mannitol powder, corresponded to a reduction in the  $T_{BET}$  of the material from 1.55 to 1.26 m<sup>2</sup>/g. This decrease in  $T_{BET}$ , also observed for the tablets made of NPMPs and CTZNa DH, was ascribed to the mechanism of fusion of particles with rising compression pressure.

Studying the compaction behaviour of lactose, Busignies et al. observed the  $T_{\text{BET}}$  of lactose to initially increase and to then decline with rising compression pressure in a similar manner to that observed for CTZNa MPs and CTZNa ANH tablets, indicating that the initial mechanism of compaction was plastic deformation and/or ductile fraction and secondly the predominant mechanism of compaction was fusion of particles<sup>18</sup>.

### **3.3. Dissolution studies**

It was postulated that the large  $T_{\text{BET}}$  of the NPMP powders preserved in the compacted tablets and the porosity of the tablets may promote faster dissolution of NPMP tablets, compared to tablets made of non-porous materials. The tablets selected for dissolution studies were those compressed at the same compression pressure of 128 MPa (Fig 8 a and c), as some of the materials did not undergo compression at lower compression pressures. Additionally, NPMP tablets investigated were also compressed at compression pressures of 64 MPa and 21 MPa (Fig. 8 b and d).

It should be noted that all dissolution studies were performed in sufficient dissolution medium to ensure sink conditions and disintegration under dissolution conditions was not observed for any of the tablets tested.



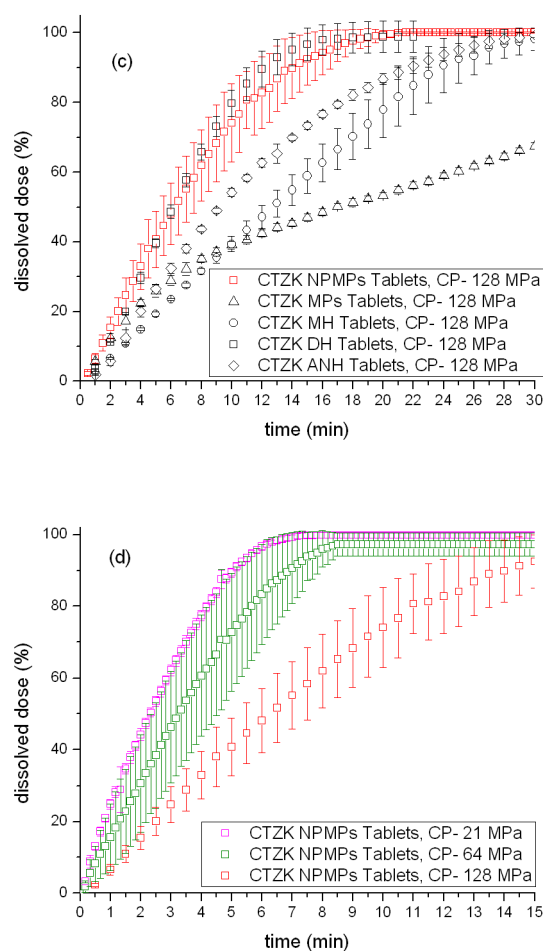


Fig. 8. Dissolution profiles ( $n \geq 3$ ) of: a) all CTZNa tablets compressed at compression pressure (CP) of 128 MPa, b) CTZNa NPMPs tablets compressed respectively at compression pressures of 21 MPa, 64 MPa and 128 MPa, c) all CTZK tablets compressed at compression pressure of 128 MPa and d) CTZNa NPMPs tablets compressed respectively at compression pressures of 21 MPa, 64 MPa and 128 MPa.

For CTZNa materials, the fastest dissolution of API was recorded for tablets made of NPMPs compressed at 21 MPa (Fig. 8 a). The  $\sigma_c$  of these tablets was 0.62 MPa, with a  $\epsilon_c$  of 64.5% which corresponded to a tablet  $T_{\text{BET}}$  of 64.7 m<sup>2</sup>/g. 100% of the 250 mg of API was dissolved between the third and fourth minute of the experiment. CTZNa NPMP tablets compressed at 64 MPa performed nearly as



well, though the standard deviations of the dissolution profile points was higher. Tablets compacted at 128 MPa had higher standard deviation (SD), ~0.6 MPa, for tablet tensile strength (4.48 MPa) than tablets compressed at lower compression pressures, indicating increased variation in tensile strength. This finding was found to correspond to increased SD in the concentration time-points of dissolution profiles. Tablets made of CTZNa NPMP prepared at a compression pressure of 128 MPa fully dissolved after 12 minutes, 7 minutes faster than CTZNa MP tablets (19 minutes). The performance of tablets made of CTZNa DH was similar to that of CTZNa MP tablets.

The CTZNa DH tablets performed better than those made of CTZNa ANH even though the latter tablets had a larger  $T_{\text{BET}}$  and  $\epsilon$ , and lower  $\sigma_i$  (SI, Table SI.1). The lower dissolution rate of CTZNa ANH can be associated with hydration and recrystallisation of CTZNa ANH to CTZNa DH, as observed by PXRD and which occurred on the tablet surface during dissolution. Similarly, lower dissolution rates, in comparison to tablets made of hydrated theophylline, were previously observed for anhydrous theophylline tablets<sup>26</sup>. This was ascribed to hydration of theophylline upon dissolution study. In the case of CTZNa ANH, 100% API was dissolved after only 30 minutes.

In the case of CTZK (Fig. 8b), the best dissolution performance was observed again for tablets made of CTZK NPMPs. As for CTZNa tablets, the tablet dissolution performance deteriorated with increasing compression pressure from 21 MPa to 128 MPa. The respective times taken to fully dissolve the tablets made of CTZK NPMPs were 6 min ( $\sigma_i$  of  $0.86 \pm 0.24$  MPa), 9 min ( $\sigma_i$  of  $2.58 \pm 0.51$  MPa) and 19 min ( $\sigma_i$  of  $5.11 \pm 0.81$  MPa). In comparison to the tablets of CTZK NPMP, the variation of the dissolution profile of CTZK DH tablets was smaller, which may be attributed to smaller deviations in  $\sigma_i$  ( $1.34 \pm 0.34$  MPa). CTZK ANH tablets were found to dissolve slower than CTZK DH, perhaps due to CTZK hydration, as was seen for CTZNa.

CTZK ANH tablets had larger  $\sigma_i$  than CTZK MH tablets and nearly 10% lower  $\epsilon$ , but compressed CTZK ANH had a  $T_{\text{BET}}$  (2.07 m<sup>2</sup>/g) twice that of CTZK MH (1.23 m<sup>2</sup>/g). Despite the differences, CTZK ANH and CTZK MH tablets fully dissolved within 30 minutes, 10 minutes slower than CTZK DH and CTZK NPMP tablets. The slowest dissolution was recorded for tablets made of CTZK MPs, which were characterised by low  $\sigma_i$  (0.93 MPa), relatively high  $\epsilon$  (32%) and  $T_{\text{BET}}$  of about 1.23 m<sup>2</sup>/g. It was observed, that for this system only about 50% of the API was dissolved up to the 30th minute.

Since the solubilities of the dihydrated salts of CTZK and CTZNa are both close to 80 mg/ml<sup>34</sup>, depicted differences in dissolution profiles can be attributed to the tablet characteristics. Amorphous, anhydrous or monohydrated forms of salts are unstable in an aqueous environment and will tend to rapidly convert to dihydrated forms which are stable in water. Direct “in situ” control of surface solid-phase transformation during dissolution experiments was not performed.

In this work, tablets with the largest  $T_{\text{BET}}$  had the fastest dissolution rates. Jaleel et al. formulated orally dispersible tablets containing loratadine from a solid dispersion with PVP K30 (1:3 w/w ratio, loratadine dose of 10 mg)<sup>26</sup>. Dissolution studies were performed at a higher rate of paddle rotation of 100 rpm than that used in this work. The tablets, considered as orally dispersible (ODTs) formulations, containing the superdisintegrant (Crospovidone- polyplasdone XL-10, polyplasdone XL) released the whole dose of loratadine after the 3<sup>rd</sup> minute and those without the superdisintegrant after the 5<sup>th</sup> minute. The results suggest that the API materials formulated as NPMPs may be considered as suitable to be formulated into ODT systems. Further studies will be undertaken to develop such formulations.

#### 4. Conclusions

Nanoparticulate microparticles (NPMP) of amorphous, anhydrous materials produced by spray drying had better tabletability performance in comparison to conventionally processed materials, as seen from single point measures of force to tensile failure ( $P$ ), tensile strength ( $\sigma$ ) and tablet porosity ( $\epsilon$ ) versus compression pressure used to compact material. The tablets made of NPMPs presented higher  $\sigma$  and higher  $\epsilon$  than those made of crystalline, non-porous spray dried material or material designed for direct compaction (Di-Pac™). The NPMP compacts partially retained large specific surface area ( $T_{\text{BET}}$ ) of the starting powders, at the same time presenting large  $\epsilon$  and satisfactory  $\sigma$ .

This study indicated that, in terms of defining the tabletability performance of compressed materials, neither particle size nor particle size distribution were critical parameters. For example, particles of the same material, such as amorphous CTZNa NPMPs and CTZNa MPs, which both had monomodal particle size distributions, very similar span values as well as very comparable  $d(10)$ ,  $d(50)$  and  $d(90)$  parameters presented very different tabletability profiles.

Salt (CTZNa and CTZK) NPMP tablets presented very good dissolution test performance indicating that NPMP materials may be considered as suitable for direct compaction and possibly for inclusion in tablet formulations as bulking agents, APIs, carriers or binders due to their good compactibility performance.

#### Acknowledgements

The authors wish to acknowledge funding for this research from Solid State Pharmaceutical Cluster (SSPC), supported by Science Foundation Ireland under grant number 07/SRC/B1158.

## Supporting Information Available

Supporting information for this manuscript is available free of charge via the Internet at

<http://pubs.acs.org/>.

## References

1. Joiris, E.; Martino, P.D.; Berneron, C.; Guyot-Hermann, A.M.; Guyot, J.C. Compression behavior of orthorhombic paracetamol. *Pharm. Res.* 1998, 15, 1122–1130.
2. Qiu, Y.; Chen, Y.; Zhang, G.G.Z.; Liu, L.; Porter W.R. *Developing Solid Oral Dosage Forms*, Elsevier Inc., USA, 2009.
3. Paluch, K.J.; Tajber, L.; McCabe, T.; O'Brien, J.E.; Corrigan, O.I.; Healy, A.M. Physicochemical analysis of crystalline chlorothiazide and chlorothiazide sodium. *Eur. J. Pharm. Sci.* 2010, 41, 603–611.
4. Paluch, K.J.; Tajber, L.; McCabe, T.; O'Brien, J.E.; Corrigan, O.I.; Healy, A.M. Preparation and characterisation of novel chlorothiazide potassium solid-state salt forms: Intermolecular self assembly suprastructures. *Eur. J. Pharm. Sci.* 2011, 42, 220–29.
5. Corrigan, O.I.; Holohan, E.M.; Sabra, K. Amorphous forms of diuretics prepared by spray drying. *Int. J. Pharm.* 1984, 18, 195–200.
6. Paluch, K.J.; Tajber, L.; Adamczyk B.; Corrigan, O.I.; Healy, A.M. A novel approach to crystallisation of nanodispersible microparticles by spray drying for improved tabletability. *Int. J. Pharm.* 2012, 15, 436 (1-2), 873-6.
7. Paluch, K.J.; Tajber, L.; Corrigan, O.I.; Healy, A.M. Impact of process variables on the micromeritic and physicochemical properties of spray-dried porous microparticles, part I: introduction of a new morphology classification system. *J. Pharm. Pharmacol.* 2012, 64(11), 1570-82.

8. Paluch, K.J.; Tajber, L.; Amaro, M.J.; Corrigan, O.I.; Healy, A.M. Impact of process variables on the micromeritic and physicochemical properties of spray-dried microparticles – Part II. Physicochemical characterisation of spray-dried materials. *J. Pharm. Pharmacol.* 2012, 64(11), 1583-91.
9. Ogáin, O.N.; Li, J.; Tajber, L.; Corrigan, O.I.; Healy, A.M. Particle engineering of materials for oral inhalation by dry powder inhalers. I – Particles of sugar excipients (trehalose and raffinose) for protein delivery. *Int. J. Pharm.* 2011, 405, 23–35.
10. Augsburger, L.L.; Hoag, S.W. *Pharmaceutical dosage forms: Tablets*, Third edition, Vol. 2 Rational design and formulation. 2008 Informa Healthcare USA Inc.
11. Sun, C.C.; Grant, D.J.W. Influence of crystal shape on the tableting performance of L-lysine monohydrochloride dihydrate. *J. Pharm. Sci.*, 2001, 90(5), 569–579.
12. Maggi, L.; Conte, U.; Bettinetti, G.P. Technological properties of crystalline and amorphous  $\alpha$ -cyclodextrin hydrates. *Int. J. Pharm.* 1998, 172, 211–217.
13. Pande, G.S.; Shangraw, R.F. Characterization of  $\beta$ -cyclodextrin for direct compression tableting: II. The role of moisture in the compactibility of  $\beta$ -cyclodextrin *Int. J. Pharm.* 1995, 124(2,3), 231-239.
14. Trasi, N.S.; Boerrigter, S.X.M.; Byrn, S.R.; Carvajal, T.M. Investigating the effect of dehydration conditions on the compactability of glucose. *Int. J. Pharm.* 2011, 406, 55–61.
15. Sebhatu, T.; Alderborn, G. Relationships between the effective interparticulate contact area and the tensile strength of tablets of amorphous and crystalline lactose of varying particle size. *Eur. J. Pharm. Sci.* 1999, 8, 235-242.
16. Di Martino, P.; Scoppa, M.; Joiris, E.; Palmieri, G.F.; Andres, C.; Pourcelot, Y.; Martelli, S. The spray drying of acetazolamide as method to modify crystal properties and to improve compression behaviour. *Int. J. Pharm.* 2001, 213, 209–221.

17. Westermarck, S.; Juppo, A.M.; Kervinen, L.; Yliruusi, Y. Pore structure and surface area of mannitol powder, granules and tablets determined with mercury porosimetry and nitrogen adsorption. *Eur. J. Pharm. Biopharm.* 1998, 46(1), 61-68.
18. Busignies, V.; Leclerc, B.; Truchon, S.; Tchoreloff, P. Changes in the specific surface area of tablets composed of pharmaceutical materials with various deformation behaviors. *Drug Dev. Ind. Pharm.* 2011, 37(2), 225-33.
19. Pitt, K.G.; Newton, J.M.; Richardson, R.; Stanley, P.; The material tensile strength of convex-faced aspirin tablets. *J. Pharm. Pharmacol.* 1989, 41(5), 289-92.
20. Es-Saheb, M.H.H. Tensile fracture characteristics of double convex-faced cylindrical powder compacts. *J. Mat. Sci.* 1996, 31(1), 214-223.
19. European Pharmacopoeia. 7th ed. (7.6), Council of Europe, Strasbourg. 2013.
21. Cobby, J.; Mayersohn, M.; Walker, G.C. Influence of shape factors on kinetics of drug release from matrix tablets II: Experimental. *J. Pharm. Sci.*, 1974, 63(5), 732 – 737.
22. Saleki-Gerhardt, A.; Ahlneck, C.; Zografi, G. Assessment of disorder in crystalline solids, *Int. J. Pharm.* 1994, 101(3), 237-247.
23. Fichtner, F.; Rasmuson, A.; Alderborn, G. Particle size distribution and evolution in tablet structure during and after compaction, *Int. J. Pharm.* 2005, 292, 211–225.
24. Sun, C.C.; Grant, D.J.W. Improved tableting properties of p-hydroxybenzoic acid by water of crystallization: a molecular insight. *Pharm. Res.* 2004, 21(2), 382- 387.
25. Haque, K.; Kawai, K.; Suzuki, T. Glass transition and enthalpy relaxation of amorphous lactose glass. *Carbohydr. Res.* 2006, 341(11), 1884-1889.
26. Debnath, S.; Suryanarayanan, R. Influence of process-induced phase transformation on dissolution of theophylline tablets. *AAPS PharmSciTech.* 2004, 5, 8.

27. Jaleel, A.; Omar, W.; Abdulrasool, Alaa, A.; Ghareeb, Mowafaq, M. Preparation and Characterization of Orally Disintegrating Loratadine Tablets from PVP Solid Dispersions. Int. J. Pharm. Sci. 2010, 2(3), 759-770.

## Table of contents

